© 2018. Published by The Company of Biologists Ltd | Journal of Experimental Biology (2018) 221, jeb191171. doi:10.1242/jeb.191171

RESEARCH ARTICLE

Ascending flight and decelerating vertical glides in Anna's hummingbirds

Victor Manuel Ortega-Jiménez[1,*] and Robert Dudley[1,2]

ABSTRACT

Hummingbirds are observationally well known for their capacity to vertically ascend whilst hovering, but the underlying mechanics and possible energetic limits to ascent rates are unclear. Decelerations during vertical ascent to a fixed target may also be associated with specific visual responses to regulate the body's trajectory. Here, we studied climbing flight and subsequent deceleration in male Anna's hummingbirds (*Calypte anna*) over an approximately 2 m vertical distance. Birds reached vertical speeds and accelerations up to ∼4 m s^{-1} and 10 m s^{-2}, respectively, through the use of flapping frequencies as high as 56 Hz and stroke amplitudes slightly greater than 180 deg. Total mass-specific power at maximal ascent speed was up to 92 W kg^{-1} body mass. Near the end of the ascending trajectory, all individuals decelerated ballistically via cessation of flapping and folding of wings over the body without losing control, a behavior termed here a vertical glide. Visual modulation of the deceleration trajectory during ascent was indicated by a constant value (∼0.75) for the first derivative of the time-to-contact to target. Our results indicate that hummingbirds in rapid vertical ascent expended near-maximal power output during flight, but also tightly controlled their subsequent deceleration during the vertical glide.

KEY WORDS: *Calypte anna*, Maximal lift, Mechanical power, Vertical climbing

INTRODUCTION

Ascending flight is commonly used by volant taxa in a diversity of biological contexts, including chases, escapes and mating behavior. Climbing animals must exert sufficient muscle power output to overcome both gravity (i.e. the potential energy gain) and aerodynamic costs, both of which will increase with increasing ascent speed. Thus, near-maximal biomechanical performance can be expected during rapid vertical flight. Although take-off and near- or fully vertical ascent has been well studied for several avian groups (see Tobalske and Dial, 2000; Askew and Marsh, 2001; Berg and Biewener, 2008; Jackson, 2009; Jackson and Dial, 2011) and for some insects (see Marden, 1987; Muijires et al., 2017), it has never been explicitly studied in hummingbirds. Nonetheless, ascending flight is well known in many trochilid taxa. For example, the curving upward trajectory of the display dive in male Anna's hummingbirds is transiently vertical near the end of the behavior (Clark, 2009). Hummingbirds more generally provide an excellent model with which to study vertical flight because, from either perches or while in stationary hovering, they can initiate high accelerations and rapidly ascend distances on the order of tens of meters. Asymptotic load-lifting studies of maximal force production in hummingbirds also indicate that they can generate total vertical forces typically ∼3 times their body weight (Chai et al., 1997; Chai and Millard, 1997; Altshuler et al., 2010), with muscle-mass-specific powers for small and large species that range from 206 to 327 W kg^{-1}, respectively. Hence, we expect that motivated unloaded hummingbirds at a maximal climbing rate should exhibit high levels of power expenditure similar to those during flight with maximal loads.

Hummingbirds in ascent must eventually slow and stop relative to global or local landmarks. When approaching a target in space, or while landing, animal fliers use exteroceptive feedback to decelerate to their final position. The function termed time-to-contact, τ (i.e. the distance-to-contact divided by the approaching speed), can be used to characterize body kinematics relative to control of the approach (see Lee, 1976). If the first derivative of τ is constant and ≤ 0.5, the trajectory will terminate at the target; if $0.5<\tau\leq 1$, then some overshooting will occur. For hummingbirds horizontally approaching a feeder, values for τ are typically 0.75, indicating a controlled but low-speed braking entrance into a simulated flower (Lee et al., 1991). Hummingbirds in ascending flight often target specific objects (e.g. flowers, small insect prey and intruders), and arrival at the target is presumably controlled visually, as in horizontal flight. Here, we analyze flight performance of Anna's hummingbirds [*Calypte anna* (Lesson 1829)] rapidly traversing a vertical distance of ∼2 m toward a nectar source, and describe their body posture and wingbeat kinematics during this feat, along with their time-to-contact function. We also document a vertical upward glide and associated body and wing orientations immediately prior to reaching their visual target.

MATERIALS AND METHODS

This research was conducted in compliance with Animal Use Protocol 2016-02-8338 at the University of California, Berkeley. Live bird trapping was carried out under permits from the United States Fish & Wildlife Service (MB054440-0) and the California Department of Fish and Wildlife (SC-6627). Four adult male Anna's hummingbirds were captured in Berkeley, CA, USA; birds were released into the wild at the capture point following the study's completion. Sample size and bird order during experimentation were based on availability, and were not fixed prior to the study so as to detect pre-specified effects. We trained each bird to perform ascending flights in a vertical chamber (2.4×0.65×0.35 m, height×width×depth) framed with PVC tubing, and covered with tulle fabric. The ceiling of the chamber consisted of white poster board; an artificial feeder filled with a commercial nectar solution (Nektar-Plus) was placed directly beneath the center of the ceiling, and a perch several centimeters above the chamber's floor. Over 2–3 days, birds were individually allowed to fly, for periods of several hours, within the chamber and to freely feed using this perch–feeder configuration.

[1]Department of Integrative Biology, University of California, Berkeley, CA 94720, USA. [2]Smithsonian Tropical Research Institute, Balboa, Republic of Panama.

*Author for correspondence (ornithopterus@gmail.com)

Received 22 August 2018; Accepted 16 October 2018

Journal of Experimental Biology (2018) 221, jeb191171. doi:10.1242/jeb.191171

List of symbols and abbreviations

A	frontal projected area
a_i	instantaneous acceleration
a_z	vertical acceleration
m_b	body mass
n	wingbeat frequency
n_{max}	maximum wingbeat frequency
P_{ind}	mass-specific induced power
$P_{kinetic}$	mass-specific kinetic power
P_{mech}	total aerodynamic power
P_{par}	mass-specific parasite power
$P_{potential}$	mass-specific potential power
P_{pro}	mass-specific profile power
R	wing length
Re	Reynolds number
S	wing area
t_c	time-to-contact
U_z	vertical speed
V_{ind}	induced velocity
z	vertical position
α_{tail}	tail orientation
β	stroke plane angle
τ	tau function
ϕ	stroke amplitude
ϕ_{max}	maximum stroke amplitude
χ_{body}	vertical body orientation

To initiate flight experiments, the feeder was first physically occluded so as to elicit perching by the bird on an additional perch inserted 30 cm above the flight chamber's floor. An array of 250 W incandescent lights was then turned on to illuminate the chamber background and ceiling, and a visual stimulus, which consisted of one of us (V.M.O.-J.) suddenly turning on the lights in an otherwise darkened room and approaching the cage while rapidly extending his arm as if to contact the bird, was used to elicit a startle response from the bird, which immediately took off and ascended vertically to the feeder. A vertical scale on one wall was used for calibration. A video camera positioned horizontally to the flight chamber, and thus with the optical axis nominally perpendicular to the flight trajectory, was used to film (at 500 frames s^{-1}) the ascent of each bird. Within the camera's field of view was also positioned a mirror (35×45 cm) placed at 45 deg from vertical so as to obtain a simultaneous recording of the trajectory from beneath the ascending bird. A single escape flight was recorded and analyzed per bird (e.g. Movie 1). Body mass m_b, wing area S and wing length R of each bird were measured after filming.

For each video sequence, the beak base, tail tip, tail base, right-wing tip and right shoulder were digitized from the lateral camera view. We also digitized the right-wing tip and right shoulder using the bottom view from the mirror. Vertical position of the bird through time (z) was obtained using the position of the beak base. Vertical body orientation, χ_{body}, was calculated as the angle from the vector formed by the beak base and tip tail with respect to the horizontal. Similarly, tail orientation (α_{tail}) was taken as the angle formed by the tail base and tip tail relative to the longitudinal body axis. A quintic spline was applied to smooth all positional data (see Walker, 1998), and the first and second derivatives of the resulting spline function were calculated to obtain the vertical speed (U_z) and acceleration (a_z), respectively. Stroke plane angle (β) relative to horizontal was calculated from the average vector formed by the wing tip at the beginning and the end of both the downstroke and the upstroke, with a correction for average vertical displacement of the body over the same time interval. For each wingbeat cycle, stroke amplitude ϕ was calculated from the vector formed by the wing tip and shoulder at the top and bottom of the wingbeat; flapping frequency n was obtained from the number of frames required to complete a wingbeat. For each recorded flight, we obtained average and maximum values of stroke amplitude and flapping frequency for all wingbeats of the ascent from the point of take-off until the bird ceased flapping and adopted a ballistic posture (see Results).

Following helicopter theory (Johnson, 1980), we estimated induced power as the product of the body weight and the sum of the bird's vertical speed (U_z) and the induced velocity (V_{ind}). Profile power was computed using the formula of Ellington (1984) and a drag coefficient equal to $7/(Re)^{0.5}$, where Re is the mean Reynolds number of the wing chord. Although this is a simplified approach to the drag coefficient (see Kruyt et al., 2014), such profile power estimates were up to ∼17% of total power requirements (see Results). Parasite power was estimated using the steady-state drag equation assuming a parasite drag coefficient equal to $2.85\times10^{-3}m_b^{0.75}/A$ (see Norberg, 1990), where A is the frontal projected area of a frozen hummingbird specimen (1.9 cm^2). Values for $P_{kinetic}$ and $P_{potential}$ were calculated as $m_bU_za_z$ and $m_bU_z\boldsymbol{g}$, respectively, where a_z is the vertical acceleration of the bird and $\boldsymbol{g}$ is the acceleration of gravity. Because $P_{potential}$ is included within the estimate of P_{ind} (see Johnson, 1980), the total aerodynamic power (P_{mech}) was estimated as the sum of $P_{kinetic}$, P_{pro}, P_{par} and P_{ind}, assuming perfect elastic storage of wing inertial energy. All mechanical power calculations were normalized by m_b, and we used the average and maximal values of U_z and a_z to calculate average and maximal values for total power output, respectively. The tau function τ was calculated as the ratio of the approach distance of the beak tip to the feeder at the start of deceleration to its instantaneous vertical speed. Instantaneous speed was estimated from the quintic spline function relating vertical position to time (see Walker, 1998). Linear fits were then determined for the relationship between the tau function and the time of contact; these fits met statistical assumptions for linear regression. A dataset including the raw data from this study is available as supplementary material (Dataset 1).

RESULTS

After take-off, birds accelerated vertically over a distance of ∼1.2 m, and then slowly decelerated (Fig. 1A–C). Mean (maximal) vertical speeds and accelerations among the four birds averaged 2.2±0.1 m s^{-1} (3.5±0.3 m s^{-1}) and 1.8±0.6 m s^{-2} (8.3±1.8 m s^{-2}), respectively (Table 1). At a height equal to ∼80% of the total ascent distance, all birds ceased flapping and folded their wings against the body while decelerating, a behavior we term a vertical glide (Fig. 1D,E; Movies 1, 2). Birds maintained this ballistic posture until they attained the approximate height of the feeder (i.e. at 2.0±0.1 m height), and then resumed flapping in hovering flight. Stroke amplitude and wingbeat frequency over the actively powered period of ascent averaged 148±19 deg and 46±2 Hz, respectively, with maxima of 181±14 deg and 53±3 Hz, respectively (Table 1). During the entire ascent (i.e. during both active and passive components), birds maintained a nearly vertical body orientation with the tail nearly parallel to the longitudinal body axis; stroke plane angle was near zero (Table 1, Fig. 1E). Values of $P_{kinetic}$, P_{pro} and P_{par} were relatively small in all cases (see Table 2). Estimates of total aerodynamic power averaged 50 W kg^{-1}, with an average maximum of 90 W kg^{-1} (see Table 2). Slopes for the first derivative of the tau function against time-to-contact averaged 0.75±0.1 among the four individual birds (Fig. 2).

Journal of Experimental Biology (2018) 221, jeb191171. doi:10.1242/jeb.191171

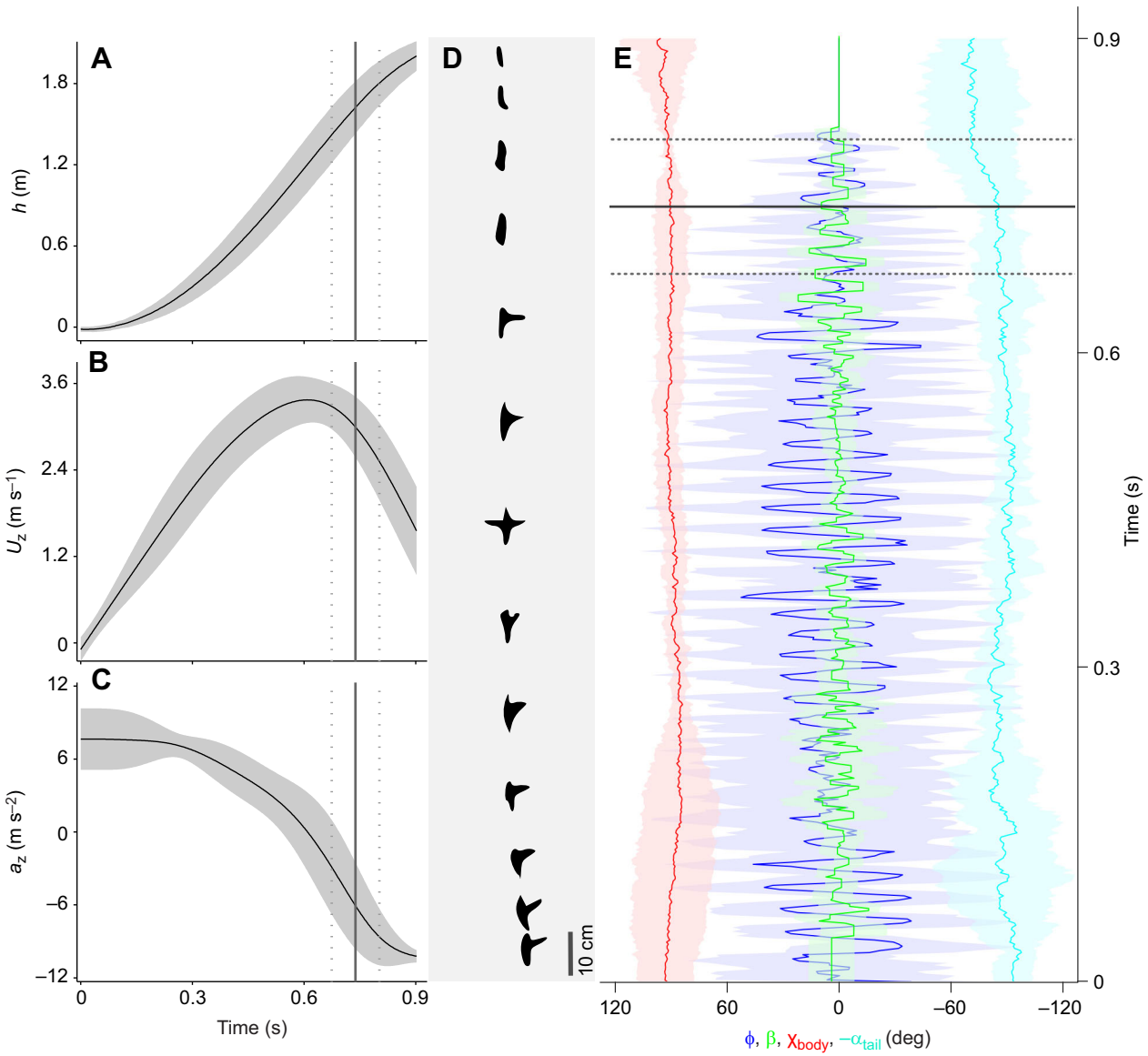

Fig. 1. Body and wing kinematics of hummingbirds in vertical ascent. (A–C) Body kinematics through time for Anna's hummingbirds (n=4) in vertical flight: (A) height, (B) vertical speed and (C) vertical acceleration; black curves and gray shaded areas represent means±1 s.d. for the four studied individuals. A single escape flight was analyzed per bird. The continuous and dotted gray vertical lines indicate the mean±1 s.d. time at which birds ceased flapping. (D) Composite image (at 64 ms intervals) of a hummingbird in vertical ascent. (E) Wingbeat kinematics and body and tail orientations through time for Anna's hummingbirds in vertical flight: ϕ (blue), stroke plane angle β (green), body angle χ_{body} (red) and tail angle α_{tail} (cyan; negatively signed for graphical clarity). Means±1 s.d. for ϕ, β, χ_{body} and α_{tail} are represented for the four studied individuals by continuous lines and shaded regions. On the ordinate of E, the continuous and broken horizontal black lines indicate the mean±1 s.d. time at which the birds stopped flapping.

DISCUSSION

During ascent from rest, Anna's hummingbirds reached speeds up to ∼4 m s^{-1} and accelerations against gravity as high as 1 ***g***. Flight performance for this behavior was comparable to that observed in studies of hummingbirds sustaining external loads of approximately one body weight, during which they hover via compensatory increases of ∼20% in both flapping frequency and wingbeat amplitude (see Chai et al., 1997; Chai and Millard, 1997). Similarly,

Table 1. Morphological parameters and kinematic results for four male Anna's hummingbirds in vertical ascent

Bird ID	m (g)	S (cm^2)	R (cm)	n (Hz)	n_{max} (Hz)	Φ (deg)	Φ_{max} (deg)	U_z (m s^{-1})	a_z (m s^{-2})	β (deg)	α_{tail} (deg)	χ_{body} (deg)
1	4.6	7.9	5.5	46	50	153	188	2.3 (3.7)	1.5 (10.1)	1.0	80	88
2	5.0	7.7	5.6	46	50	147	183	2.1 (3.3)	2.5 (6.2)	−0.2	88	86
3	4.7	7.2	5.6	45	56	145	180	2.3 (3.2)	1.1 (9.5)	0.5	94	94
4	5.5	8.0	5.7	49	56	145	174	2.3 (3.7)	2.1 (7.5)	−0.1	81	90
Mean	5.0	7.7	5.6	46	53	148	181	2.2 (3.5)	1.8 (8.3)	0.3	86	90
s.d.	0.4	0.4	0.1	2	3	4	5	0.1 (0.3)	0.6 (1.8)	0.6	7	3

See List of symbols and abbreviations for definitions. Maximum values for vertical velocity and acceleration are given in parentheses.

Journal of Experimental Biology (2018) 221, jeb191171. doi:10.1242/jeb.191171

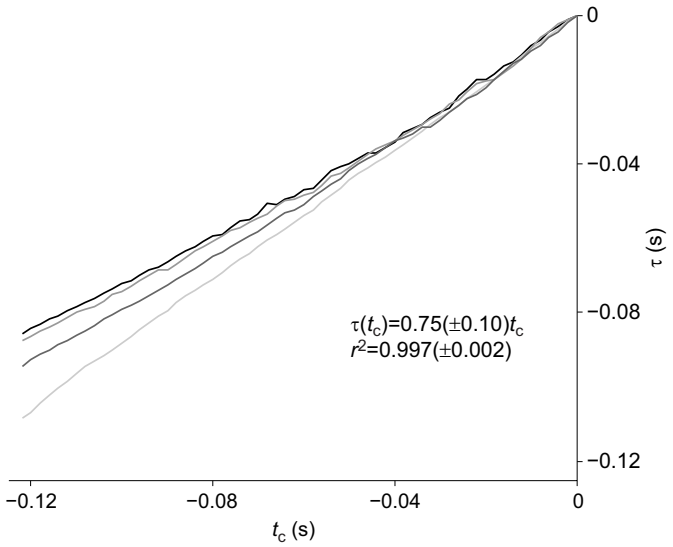

Fig. 2. Values of the tau function versus time-to-contact for four ascending Anna's hummingbirds during deceleration. The inset linear regression is derived from all pooled data. Equations for individual birds are as follows: bird 1, $\tau(t_c)=0.69t_c–0.004$ ($r^2=0.99$, $P<0.0001$); bird 2, $\tau(t_c)=0.87t_c–0.001$ ($r^2=0.99$, $P<<0.001$); bird 3, $\tau(t_c)=0.71t_c–0.004$ ($r^2=0.99$, $P<0.0001$); bird 4, $\tau(t_c)=0.76t_c–0.004$ ($r^2=0.99$, $P<0.0001$). A single escape flight was recorded and analyzed per bird.

Anna's hummingbirds during ascent showed average (maximal) increases in n and ϕ of 13% (29%) and 17% (44%), respectively (see Table 1), relative to typical values in hovering flight (i.e. 41 Hz and 126 deg, respectively; Ortega-Jimenez and Dudley, 2012). Body-mass-specific power P_{per} (i.e. $P_{pro}+P_{par}+P_{ind}$) of these ascending hummingbirds averaged 48 W kg^{-1}, which corresponds to ∼185 W kg^{-1} of muscle-mass-specific power output assuming a flight muscle to body mass fraction of 26% (the average value from 14 species of hummingbirds obtained by Altshuler et al., 2010). This latter power estimate is 41% greater than that estimated for comparably sized ruby-throated hummingbirds hovering in a demanding low-density atmosphere (∼131 W kg^{-1}; Chai and Dudley, 1996). By contrast, the average muscle-mass-specific power value of ascending hummingbirds was up to 24% lower than that of small hummingbird species (<4 g) lifting maximum loads over a shorter time period (i.e. 206–230 W kg^{-1} of muscle; Chai et al., 1997; Chai and Millard, 1997). However, direct comparison of load-lifting studies and the vertical ascent described here is confounded, as hummingbirds in the present study exhibited variable accelerations and changes in potential energy during the behavior, and power estimates will thus strongly depend on the time interval of estimation. Our calculations do suggest, however, that the total maximum muscle-mass-specific power of Anna's hummingbirds, which includes $P_{kinetic}$ and $P_{potential}$, can be as high as 354 W kg^{-1} (see Table 2); this value is ∼10% higher than that achieved by large hummingbirds (∼8 g) lifting three times their body mass (∼327 W kg^{-1}; Chai and Millard, 1997). Black-chinned hummingbirds during much more rapid transient maneuvers can reach values of ∼480 W kg^{-1} of muscle mass (see Cheng et al., 2016). Here, the motivated vertical ascent in question occurs over 40–45 wingbeats, and is thus behaviorally very different than sustained hovering in low-density gas mixtures (Chai and Dudley, 1996), but more similar (albeit still of longer duration) to those during territorial bouts (e.g. Sholtis et al., 2015). Thus, physiological limits to hummingbird flight performance in different kinds of challenging scenarios (e.g. flight in reduced atmospheres, maneuvers or accelerating ascent) may reflect time-dependent aerobic performance of the flight muscle under such conditions (see Butler, 2016). During vertical escape, songbirds of mass <10 g are characterized by average mass-specific power outputs ranging from 90 to 100 W kg^{-1} (see fig. 7 in Jackson, 2009), values that are similar to those obtained here for hummingbirds in vertical ascent (Table 2).

Table 2. Mean mass-specific power components and total power for male Anna's hummingbirds in vertical ascent

Bird ID	$P_{kinetic}$	$P_{potential}$	P_{pro}	P_{par}	P_{ind}	P_{mech}
1	0.5 (20)	23 (36)	8 (16)	1 (5)	39 (51)	49 (92)
2	2.8 (11)	20 (32)	7 (14)	1 (4)	37 (47)	48 (76)
3	0.6 (16)	22 (31)	7 (19)	1 (3)	39 (46)	48 (84)
4	1.9 (19)	22 (36)	7 (15)	1 (5)	40 (52)	50 (91)
Mean	1.5 (17)	22 (34)	7 (16)	1 (4)	39 (49)	49 (86)
s.d.	1.1 (4)	1 (3)	1 (2)	0 (1)	1 (3)	1 (7)

All units are W kg^{-1}; maximal values are given in parentheses. $P_{kinetic}$, mass-specific kinetic power; $P_{potential}$, mass-specific potential power; P_{pro}, mass-specific profile power; P_{par}, mass-specific parasite power; P_{ind}, mass-specific induced power; P_{mech}, total aerodynamic power.

Power production during vertical flight has also been studied in larger birds. For example, various phasianid species (e.g. chukar and bobwhite quail) can produce a muscle power output of ∼150 W kg^{-1} in vertical ascent (Tobalske and Dial, 2000), roughly half that of the hummingbirds studied here. Similarly, corvids and quail during vertical burst escape reach high and likely maximal muscle-specific powers ranging from 200 to 471 W kg^{-1} of muscle (Jackson and Dial, 2011; Askew and Marsh, 2001). Hummingbirds in the present study in vertical ascent reached power outputs comparable to the average values reached by the aforementioned larger birds, in part because of high stroke amplitudes and flapping frequencies (see Table 1); these power estimates suggests a vertical speed limit for male Anna's hummingbirds of approximately ∼4 m s^{-1} in still air. However, the maximal muscle power output of hummingbirds as estimated here may also reflect the absence of anaerobic contributions, which will be present in the larger avian taxa. Additional studies of ascending flight over short distances can potentially demonstrate limiting kinematics and the mechanical costs of maximum performance for a variety of volant taxa, including insects and bats, and without the use of external weight loading, altered flight media or other such experimental manipulations.

Ascending hummingbirds accelerate maximally during the initial portion of the ascent, and then progressively slow (Fig. 1C). As observed in horizontal deceleration to feeders (Lee et al., 1991), the rate of slowing is consistent with use of the tau function, although in this case target approach occurs during passive upward gliding with folded wings. Substantial wing folding and bending (also known as wing morphing) is known from swifts in gliding maneuvers (Lentink et al., 2007), during intermittent flights in some avian taxa (Tobalske et al., 2009) and during passage through apertures (Schiffner et al., 2014), although the timing of wing folding relative to body trajectories has not been examined in these cases. Particularly impressive here is the calculated ballistic approach to the top of the flight chamber, with wing folding occurring approximately 150 ms prior to the end of the trajectory (Fig. 1). Control of body pitch (either passively or actively) is also required to maintain vertical posture; corrective torque could be applied either aerodynamically or inertially through tail motions (see Movies 1, 2). Comparable use of the tail, apparently for stability, occurs in Anna's hummingbirds during horizontal flight in von Kármán vortex streets (Ortega-Jimenez et al., 2014). Impressively, hummingbirds in

vertical ascent are also capable of controlled high-speed shaking (Movie 3), a behavior otherwise only known during hovering in rain (Ortega-Jimenez and Dudley, 2012; this aerial shaking sequence was not included in either the data tables or power estimates). Such precise positional control during rapid ascent, as well as the vertical glide, further extend the range of novel maneuvers (see also Dakin et al., 2018) that have been recently described for this amazing lineage of birds.

Acknowledgements
We thank Sarahi Arriaga-Ramirez for programming help in MATLAB.

Competing interests
The authors declare no competing or financial interests.

Author contributions
Conceptualization: V.M.O.-J., R.D.; Methodology: V.M.O.-J., R.D.; Software: V.M.O.-J.; Validation: V.M.O.-J.; Formal analysis: V.M.O.-J.; Investigation: V.M.O.-J., R.D.; Resources: R.D.; Data curation: V.M.O.-J.; Writing - original draft: V.M.O.-J., R.D.; Writing - review & editing: V.M.O.-J., R.D.; Visualization: V.M.O.-J.; Supervision: V.M.O.-J., R.D.; Project administration: R.D.; Funding acquisition: R.D.

Funding statement
This work was supported by the National Science Foundation (DGE-0835290).

Supplementary information
Supplementary information available online at
http://jeb.biologists.org/lookup/doi/10.1242/jeb.191171.supplemental

References

Altshuler, D. L., Dudley, R., Heredia, S. M. and McGuire, J. A. (2010). Allometry of hummingbird lifting performance. *J. Exp. Biol.* **213**, 725-734.
Askew, G. N. and Marsh, R. L. (2001). The mechanical power output of the pectoralis muscle of the blue breasted quail (*Coturnix chinensis*): the *in vivo* length cycle and its implications for muscle performance. *J. Exp. Biol.* **204**, 3587-3600.
Berg, A. M. and Biewener, A. A. (2008). Kinematics and power requirements of ascending and descending flight in the pigeon (*Columba livia*). *J. Exp. Biol.* **211**, 1120-1130.
Butler, P. (2016). The physiological basis of bird flight. *Phil. Trans. R. Soc. B* **371**, 20150384.
Chai, P. and Dudley, R. (1996). Limits to flight energetics of hummingbirds hovering in hypodense and hypoxic gas mixtures. *J. Exp. Biol.* **199**, 2285-2295.
Chai, P. and Millard, D. (1997). Flight and size constraints: hovering performance of large hummingbirds under maximal loading. *J. Exp. Biol.* **200**, 2757-2763.
Chai, P., Chen, J. S. C. and Dudley, R. (1997). Transient hovering performance of hummingbirds under conditions of maximal loading. *J. Exp. Biol.* **200**, 921-929.
Cheng, B., Tobalske, B. W., Powers, D. R., Hedrick, T. L., Wang, Y., Wethington, S. M., Chiu, G. T. C. and Deng, X. (2016). Flight mechanics and control of escape manoeuvres in hummingbirds II. Aerodynamic force production, flight control and performance limitations. *J. Exp. Biol.* **219**, 3532-3543.
Clark, C. J. (2009). Courtship dives of Anna's hummingbird offer insights into flight performance limits. *Proc. R. Soc. Lond. B.* **276**, 3047-3305.
Dakin, R., Segre, P. S., Straw, A. D. and Altshuler, D. L. (2018). Morphology, muscle capacity, skill, and maneuvering ability in hummingbirds. *Science* **359**, 653-657.
Ellington, C. P. (1984). The aerodynamics of hovering insect flight. VI. Lift and power requirements. *Phil. Trans. R. Soc. Lond. B* **305**, 145-181.
Jackson, B. E. (2009). The allometry of bird flight performance. *PhD thesis*, University of Montana.
Jackson, B. E. and Dial, K. P. (2011). Scaling of mechanical power output during burst escape flight in the Corvidae. *J. Exp. Biol.* **214**, 452-461.
Johnson, W. (1980). *Helicopter Theory*. New York: Dover Publications, Inc.
Kruyt, J. W., Quicazán-Rubio, E. M., van Heijst, G. F., Altshuler, D. L. and Lentink, D. (2014). Hummingbird wing efficacy depends on aspect ratio and compares with helicopter rotors. *J. R. Soc. Interface* **11**, 20140585.
Lee, D. N. (1976). A theory of visual control of braking based on information about time-to-collision. *Perception* **5**, 437-459.
Lee, D. N., Reddish, P. E. and Rand, D. T. (1991). Aerial docking by hummingbirds. *Naturwissenschaften* **78**, 526-527.
Lentink, D., Müller, U. K., Stamhuis, E. J., De Kat, R., Van Gestel, W., Veldhuis, L. L. M., Henningsson, P., Hedenström, A. and Van Leeuwen, J. L. (2007). How swifts control their glide performance with morphing wings. *Nature* **446**, 1082-1085.
Marden, J. H. (1987). Maximum lift production during takeoff in flying animals. *J. Exp. Biol.* **130**, 235-238.
Muijires, F. T., Chang, S., van Veen, W., Spitzen, J., Biemans, B. T., Koehl, M. A. R. and Dudley, R. (2017). Escaping blood-fed malaria mosquitoes minimize tactile detection without compromising on take-off speed. *J. Exp. Biol.* **220**, 3751-3762.
Norberg, U. M. (1990). *Vertebrate Flight: Mechanics, Physiology, Morphology, Ecology and Evolution*. Berlin: Springer-Verlag.
Ortega-Jimenez, V. M. and Dudley, R. (2012). Flying in the rain: hovering performance of Anna's hummingbirds under varied precipitation. *Proc. R. Soc. Lond. B* **279**, 3996-4002.
Ortega-Jimenez, V. M., Sapir, N., Wolf, M., Variano, E. A. and Dudley, R. (2014). Into turbulent air: size-dependent effects of von Kármán vortex streets on hummingbird flight kinematics and energetics. *Proc. R. Soc. Lond. B* **281**, 20140180.
Schiffner, I., Vo, H. D., Bhagavatula, P. S. and Srinivasan, M. V. (2014). Minding the gap: in-flight body awareness in birds. *Front. Zool.* **11**, 64.
Sholtis, K. M., Shelton, R. M. and Hedrick, T. L. (2015). Field flight dynamics of hummingbirds during territory encroachment and defense. *PLoS ONE* **10**, 125659.
Tobalske, B. W. and Dial, K. P. (2000). Effects of body size on take-off flight performance in the Phasianidae (Aves). *J. Exp. Biol.* **203**, 3319-3332.
Tobalske, B. W., Hearn, J. W. D. and Warrick, D. R. (2009). Aerodynamics of intermittent bounds in flying birds. *Exp. Fluids.* **46**, 963-973.
Walker, J. A. (1998). Estimating velocities and accelerations of animal locomotion: a simulation experiment comparing numerical differentiation algorithms. *J. Exp. Biol.* **201**, 981-995.

Dataset 1. Morphometric information and digitization in 2D of hummingbirds (*N*=4) during ascending flight. Scale 395.22 pixels/m. Tail tip (Pt1), right-wing tip in mirror (Pt2), right-wing base in mirror (Pt3), beak base (Pt4), left-wing base in mirror(Pt5) and tail base (Pt6)

Click here to Download Dataset 1

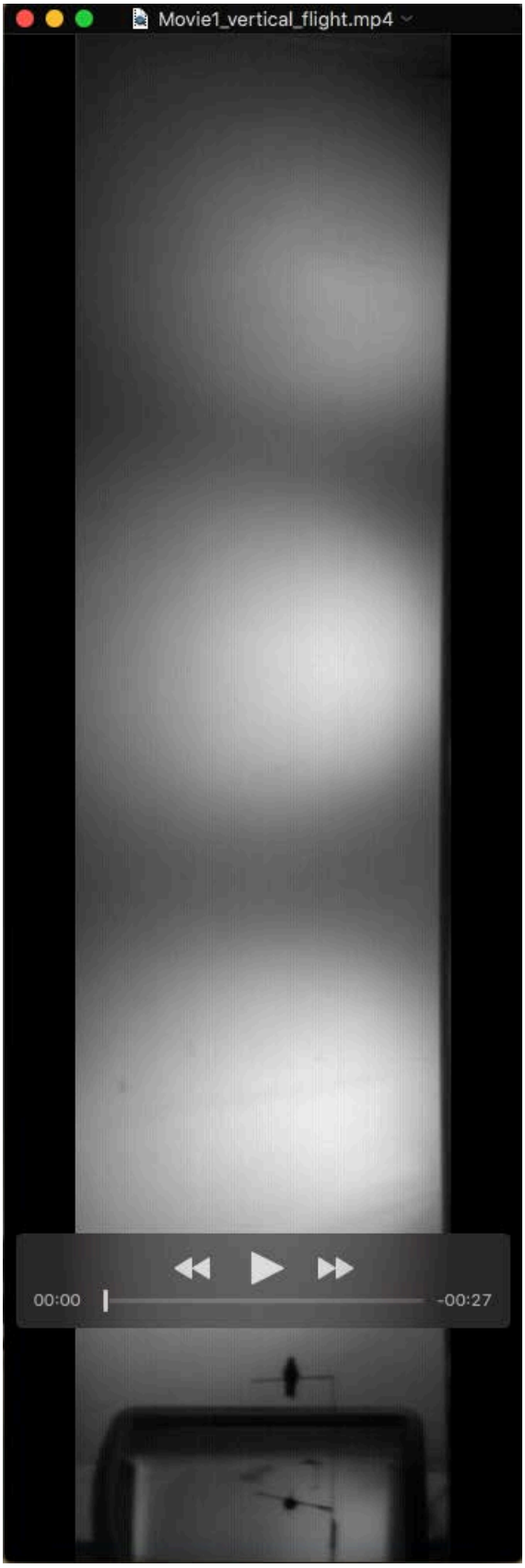

Movie 1. Anna's hummingbird in vertical ascent.

Movie 2. Ascending Anna's hummingbird adopting a ballistic posture with folded wings upon cessation of flapping.

Movie 3. Anna's hummingbird shaking its body and changing wing phase relationships while in vertical ascent.